Hindawi Publishing Corporation
Journal of Sensors
Volume 2016, Article ID 2390734, 8 pages
http://dx.doi.org/10.1155/2016/2390734

Research Article

A UEP LT Codes Design with Feedback for Underwater Communication

Danfeng Zhao, Jie Wen, and Jiaxi Si

College of Information and Communication Engineering, Harbin Engineering University, Harbin, China

Correspondence should be addressed to Jie Wen; wenjie_wsq@126.com

Received 25 March 2016; Accepted 1 August 2016

Academic Editor: Vincenzo Stornelli

To satisfy the performance requirement of LT codes with Unequal Erasure Protection (UEP) in underwater environment, the Weighted Expanding Window Fountain (WEWF) code is proposed in this paper. The WEWF codes can achieve strong UEP property by nonuniformly selecting input symbols within each window. To overcome the disadvantages in terms of redundancy in the lower prioritized segments, Correlation Chain Feedback (CCFB) is also introduced to help the transmitter to precisely adjust the encoding scheme. Asymptotic analysis and simulation results demonstrate that the proposed approach can achieve lower symbol error rate and less overall redundancy in the underwater acoustic sensor networks.

1. Introduction

Up to now, digital fountain codes (DFC) have become an efficient data transmission scheme for underwater acoustic sensor networks (UASNs) [1–3], and the most commonly used DFC are LT codes and Raptor codes. LT codes are the first realization of DFC and have the characteristic of low computation complexity [4]; at the same time, Raptor codes can achieve linear-time encoding and decoding by the concatenation of LT codes with other precoding schemes [5]. In general, LT codes are designed to provide equal erasure protection (EEP) for all input symbols. However, for some applications like underwater image transmission with MPEG or H.264 compression technique, a portion of data may need more protection than the rest. To satisfy the requirements of such applications, the codes with Unequal Erasure Protection (UEP) were proposed [6].

Choosing a degree according to a degree distribution and uniformly selecting input symbols as neighbors are two core steps of LT encoding. Existing UEP LT coding methods can be divided into two categories, the first of which is to change the selecting probability to guarantee that higher prioritized segments can get more protection, such as Weighted LT (WLT) codes [7] and Expanding Window Fountain (EWF) codes [8]. And the second, such as the duplication method proposed in [9] and Duplicating-Expanding Window Fountain (D-EWF) codes [10], is based on the idea of virtually increasing the source block size. The latter is more superior in terms of UEP performance, however, at the cost of compromising quite big transmission budget once the original source block size or repeat factors are large. Although the aforementioned methods successfully provide UEP, there still exists a significant price in terms of redundancy especially for the lower prioritized segments.

A feasible method to solve this problem is to introduce intermediate feedback into UEP LT codes [11, 12], improving the decoding performance of the lower prioritized segments [13–15] dramatically. Therefore, this paper proposes an efficient solution to provide UEP for energy-restricted underwater environment with harsh channel conditions by utilizing the abovementioned method to improve the performance of the more important data and simultaneously introducing the Correlation Chain Feedback to optimize the overall redundancy.

The rest of this paper is organized as follows. Section 2 describes the design and provides an asymptotic analysis of the proposed method. Section 3 presents the simulation results, and this paper is concluded in Section 4.

2. Weighted Expanding Window Fountain Codes

In this section, we firstly propose a new method called Weighted Expanding Window Fountain (WEWF) codes; it improves the UEP performance of EWF codes by introducing weighted scheme into the lower prioritized windows. After that, the asymptotic analysis of the proposed method is given. Finally, we bring in Correlation Chain Feedback to optimize the performance of the lower prioritized segments.

2.1. Weighted Expanding Window Fountain. Suppose that a source block of K symbols is partitioned into r adjacent classes $S_1, S_2, \ldots, S_r$ of size $\alpha_1 K, \alpha_2 K, \ldots, \alpha_r K$, where α_i is the proportion of the ith prioritized class accounted for by the source data with $\sum_{m=1}^{r} \alpha_m = 1$. Noticeably, the important level of Si decreases with the increase of i. Two parameters also are defined as $A(x) = \sum_{m=1}^{r} \alpha_m x^m$ and $\Theta_i = \sum_{m=1}^{i} \alpha_m$. Firstly, we divide these classes into r windows $w_1, w_2, \ldots, w_r$, and each window w_i can be written as the concatenation of the classes $S_1, S_2, \ldots, S_i$ with the size of the ith window satisfying $|w_i| = \sum_{m=1}^{i} \alpha_m K$. A degree distribution on the set $\{1, 2, \ldots, |w_i|\}$ is defined as $\Omega^{(i)}(x) = \sum_{m=1}^{|w_i|} \Omega_m^{(i)} x^m$; then, the proposed Weighted Expanding Window Fountain (WEWF) codes can be generated as follows:

(1) Randomly select a window based on a probability distribution $\Gamma(x) = \sum_{m=1}^{r} \Gamma_m x^m$ such that Γ_i is the probability of the selected window i.

(2) Randomly select a degree $d \in \{1, 2, \ldots, |w_i|\}$ according to the degree distribution $\Omega^{(i)}(x)$.

(3) Suppose that the weighted vector of the ith window is $B^{(i)} = \sum_{m=1}^{i} k_m^{(i)} x^m$, where $\sum_{m=1}^{i} k_m^{(i)} \alpha_m = \Theta_i$. Choose uniformly d distinct input symbols as neighbors if they satisfy $i = 1$. Otherwise, the adjacent input symbols are determined nonuniformly at random. As for any source block S_m, we choose d_m distinct input symbols with $d_m = \min([\alpha_m d k_m^{(i)}], \alpha_m K)$, and the last $d_i = d - \sum_{m=1}^{i-1} d_i$ neighbors are chosen from S_i. Here, the operator $[x]$ means the nearest integer to x.

(4) Finally, the output symbols are generated by the operation of the bitwise modulo-2 sum of the neighbors.

To summarize, WEWF code denoted by $\Psi_{\text{WEW}}(A, \Gamma, B^{(1)}, \ldots, B^{(r)}, \Omega^{(1)}, \ldots, \Omega^{(r)})$ is a fountain code which assigns each output symbol to the ith window with probability Γ_i and encodes the chosen window with distribution $\Omega^{(i)}(x)$ using WLT code with weighted vector $B^{(i)}$. The coding process can be illustrated well in Figure 1.

As shown in Figure 2, the input symbols are partitioned into two adjacent classes including a set of More Important Symbols (MIS) S_1 and a set of Less Important Symbols (LIS) S_2, whereas these two classes of data can be divided into two windows. For example, the window w_1 includes class S_1 and the window w_2 consists of all input symbols. Suppose that the weighted vector of w_2 is $B = \{k_M, k_L\}$, and the selected probabilities of S_1 and S_2 are $\eta_M = k_M/K$ and $\eta_L = k_L/K$, respectively. The degree distributions for w_1 and w_2 are defined as $\Omega^{(1)}(x) = \Omega_{rs}(\alpha_1 K, c, \delta)$ and $\Omega^{(2)}(x) = \Omega_{rs}(K, c, \delta)$.

2.2. Asymptotic Analysis of WEWF Codes. Denote ε as the reception overhead of WEWF codes and we derive the asymptotic erasure probabilities after l iterations using the iterative BP decoding algorithm for the input symbols of different classes. The original And-Or trees analysis [16] was already generalized for the weighted approach and extended for the expanding window scheme, where both different classes of OR nodes and AND nodes are introduced [17]. Similarly, we further generalize the And-Or trees construction by introducing different OR nodes selection probability within each selection window and derive the And-Or trees lemma for WEWF codes.

To the best of our knowledge, the asymptotic degree distribution of the output symbols for the jth class is $\Omega^{(j)}(x)$ and $\mu_j = \Omega^{(j)\prime}(1)$ denotes the average degree of the output symbols. For EWF codes, the set of the input symbol degree distributions is

$$\Lambda^{(j)}(x) = P\left[\sum_{l=m}^{r} \mu_l \left(\Gamma_l (1+\varepsilon) K\right) \frac{1}{\Theta_l K} (x-1)\right], \quad (1)$$

where $P(x)$ is the Poisson distribution. The average size of the lth class is $\Gamma_l(1+\varepsilon)K$, and $1/\Theta_l K$ is the probability that an OR node is chosen to be a child of an AND node from the class. As for WEWF codes, let $\eta_j^{(m)} = k_j^{(m)}/\Theta_m K$ denote the probability that an OR node from class is chosen to be a child of an AND node from the class; then the input symbol degree distribution of the WEWF is given by

$$\begin{aligned}\Phi^{(j)}(x) &= P\left[\sum_{l=m}^{r} \mu_l \left(\Gamma_l (1+\varepsilon) K\right) \eta_j^{(l)} (x-1)\right] \\ &= P\left[(1+\varepsilon) \sum_{l=j}^{r} \frac{\mu_l \Gamma_l k_j^{(l)}}{\Theta_l} (x-1)\right].\end{aligned} \quad (2)$$

For EWF codes, the generalized And-Or tree $\text{GT}_{l,j}$ is constructed using r different classes of both AND and OR nodes. Suppose that the root node of $\text{GT}_{l,j}$ is an OR node of the mth class and the tree has a depth of $2l$. Each AND or OR node from the mth class has i children with probabilities of $\beta_{i,m}$ or $\delta_{i,m}$. Furthermore, an AND node from the mth class can only have OR node children belonging to the classes $\{1, 2, \ldots, m\}$, with the associated probabilities of choosing children from the different OR classes being $\{q_1^{(m)}, q_2^{(m)}, \ldots, q_m^{(m)}\}$, and an OR node from the mth class can only have AND node children from classes $\{m, m+1, \ldots, r\}$ with the associated class probabilities $\{p_m^{(m)}, p_{m+1}^{(m)}, \ldots, p_r^{(m)}\}$. Let the nodes from the mth class at the tree depth $2l$ be initialized as 0 with probability of $y_{0,m}$ and 1 otherwise. We assume that OR nodes with no children have a value of 0, whereas AND nodes with no children have a value of 1. We quote the following generalized version of the And-Or trees lemma from [6].

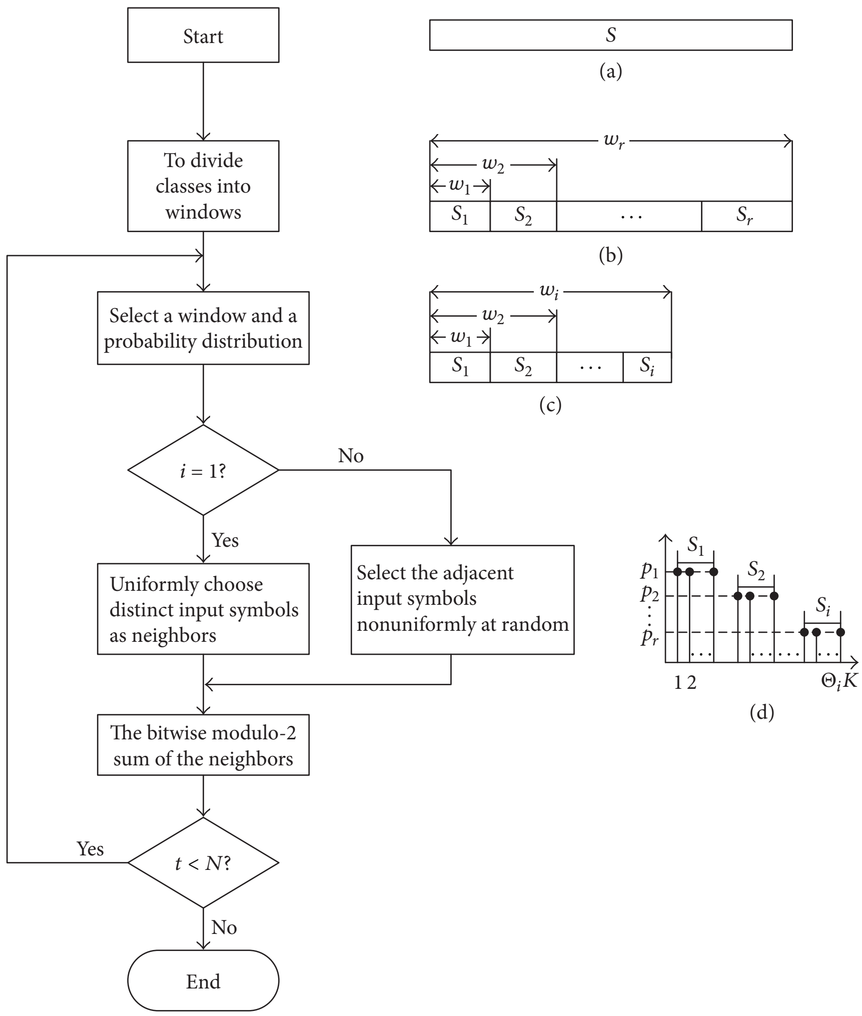

Figure 1: Flow of WEWF codes.

Lemma 1. *Let $y_{l,j}$ be the probability that the root of an And-Or tree is evaluated at 0; that is,*

$$y_{l,j} = \delta_j\left[1 - \sum_{i=j}^{r} p_i^{(j)}\beta_i\left(1 - \sum_{m=1}^{i} q_m^{(i)} y_{l-1,m}\right)\right] \tag{3}$$

with $\delta_j(x) = \sum_i \delta_{i,j}x^i$ and $\beta_j(x) = \sum_i \beta_{i,j}x^i$. Similar to the derivation in [5], $\beta_{i,j}$ is the probability that the output symbol connected with a randomly selected edge has degree $i+1$ given that it belongs to the class j, satisfying $\beta_{i,j} = (i+1)\Omega_{i+1}^{(j)}/\Omega^{(j)\prime}(1)$ with $\beta_j(x) = \Omega^{(j)\prime}(x)/\mu_j$. Similarly, $\delta_{i,j}$ is the probability that the input symbol connected with a randomly selected edge, which belongs to class j and has degree $i+1$, equals $\delta_{i,j} = (i+1)\Phi_{i+1}^{(j)}/(1+\varepsilon)\sum_{l=j}^{r}(\mu_l\Gamma_l k_j^{(l)}/\Theta_l)$, so we achieve $\delta_j(x) = \exp[(1+\varepsilon)\sum_{l=j}^{r}(\mu_l\Gamma_l k_j^{(l)}/\Theta_l)(x-1)]$. For the class m input symbols, the probability of having class output symbol as a child, $m \le j \le r$, equals $p_j^{(m)} = (\mu_j\Gamma_j k_m^{(j)}/\Theta_j)/\sum_{l=m}^{r}(\mu_l\Gamma_l k_m^{(l)}/\Theta_l)$. Similarly, the class m output symbols have the class j input symbol children, $1 \le j \le m$, with probability of $q_j^{(m)} = k_j^{(m)}\alpha_j/\Theta_m$.

Lemma 2. *For a WEWF code $\Psi_{WEW}(A, \Gamma, B^{(2)}, \dots, B^{(r)}, \Omega^{(1)}, \dots, \Omega^{(r)})$, the probability $y_{l,j}$ that the input symbol of class j is not recovered after l iterations of BP algorithm at the reception overhead ε is*

$$y_{0,j} = 1;$$

$$y_{l,j} = \exp\left[-(1+\varepsilon) \cdot \sum_{i=j}^{r}\frac{k_j^{(i)}\Gamma_i}{\Theta_i}\Omega^{(i)\prime}\left(1 - \sum_{m=1}^{i}\frac{k_m^{(i)}\alpha_m}{\Theta_i}y_{l-1,m}\right)\right]. \tag{4}$$

2.3. Correlation Chain Feedback. The performance improvement of More Important Symbols (MIS) is notable, however, at the cost of performance degradation on Less Important Symbols (LIS) compared with the EWF codes. In view of this, a feedback scheme is introduced in this section to solve this problem. Traditional feedback message contains the number of input symbols that have already been recovered

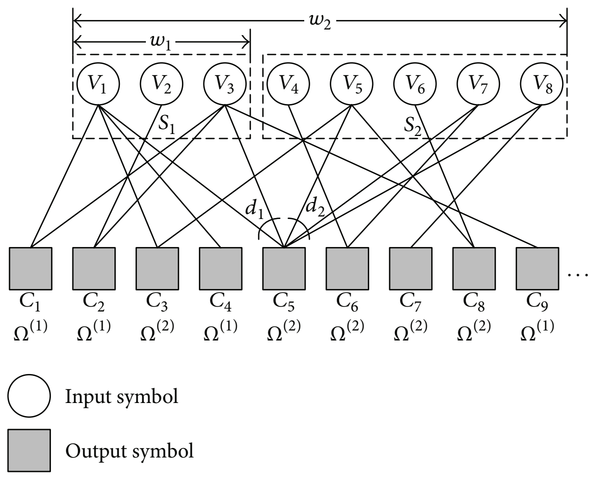

Figure 2: Process of WEWF codes including two important levels of data.

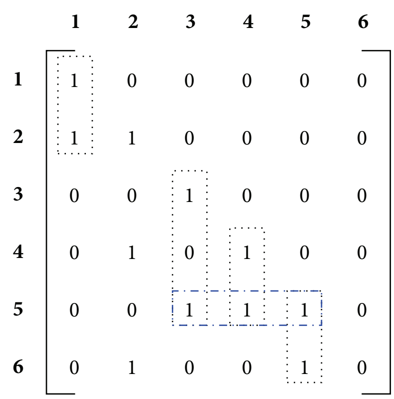

Figure 3: The extraction process of the Correlation Chain (CC).

while ignoring the information remaining in the updated generation matrix $\mathbf{G}'$. So we define Correlation Chain (CC) to describe this information.

Definition 3 (correlation pair). For $\mathbf{G}'$, a correlation pair of CP(j) is defined as a sequence, $\{c_1^{(j)}, c_2^{(j)}\}$, consisting of locations of the rows where the value is 1 in the jth column of degree 2.

As illustrated in Figure 3, for example, there are four correlation pairs of related numbers which are CP(1) = {1, 2}, CP(2) = {3, 5}, CP(3) = {4, 5}, and CP(4) = {5, 6}; there exists a common element for CP(2) = {3, 5}, CP(3) = {4, 5}, and CP(4) = {5, 6} so that all of them make up a Correlation Chain (CC), namely, {3, 4, 5, 6}. Due to the inexistence of a common element for CP(1) = {1, 2}, it itself forms a chain of CC. In other words, two chains of CC can be attained, that is, {1, 2} and {3, 4, 5, 6}. Through the extraction process of CC, it is clear that once any input symbol corresponding to the elements in CC is recovered, other corresponding symbols also can be decoded.

Therefore, this paper transfers both traditional feedback messages and CC, that is, Correlation Chain Feedback (CCFB), to the encoder when the MIS are fully recovered or the decoding process is interrupted before successfully decoding. Once the CCFB is obtained, the input symbols can be divided into the following categories, with descending priorities: (1) symbols corresponding to the first element of CC; (2) uncovered symbols of MIS; (3) other uncovered symbols; (4) symbols corresponding to other elements of the CC; (5) symbols that have been recovered. Utilizing a nonuniformly selecting scheme, the higher prioritized symbols would participate in the encoding process with higher probability.

3. Simulation Results and Analysis

The simulation is performed from two aspects: one is based on VS2010 to test and verify the performance of WEWF codes and the other is established on OPNET modeler in order to demonstrate that the proposed scheme is suitable for UASNs.

Simulations are firstly carried out by VS2010; the number of input symbols of size $K = 1000$ is partitioned into two prioritized segments, whereas the MIS block consists of the first 10% input symbols. The RSD using the degree distribution of $c = 0.03$, $\delta = 0.5$, and the MIS window with the selection probability of $\Gamma_1 = 0.23$ are considered for visual analysis.

Symbol Erasure Rate (SER). Figure 4 shows comparison of Symbol Erasure Rate (SER) of both MIS and LIS varied with overhead for all three kinds of UEP LT codes including the proposed WEWF codes with weighted factor $k_m = 1.2$, EWF codes, and WLT codes with parameter $k_m = 1.86$. The channel is recognized as lossless. It more clearly appears that, for MIS, WEWF codes can achieve the reception overhead $\varepsilon = -0.05$ at the SER of 10^{-3}, compared to the EWF and WLT codes with 0.05 and 0.17, respectively. Besides, under the condition of $\varepsilon = 0.25$, the SER of WLT codes is the lowest which equals 2.083×10^{-6}, while the WEWF codes have a SER of 9×10^{-6} followed by EWF codes with SER of 1.458×10^{-5}. Noticeably, our method can provide better performance for MIS compared to EWF and WLT codes for the scenario of the reception overhead $\varepsilon < 0.23$.

Considering the harsh underwater communication conditions, the influence of Packet Loss Rate (PLR) on the performance of UEP LT codes cannot be ignored. Figure 5 depicts the SER performance comparison versus PLR for three investigated UEP LT codes. It is shown that their SER seem to be comparable when the PLR is below 0.3. As the PLR continues to increase, the SER of WEWF codes decline rapidly, and the SER of EWF codes start to decrease until $\varepsilon = 0.325$. Though EWF codes provide better performance for the range of PLR from 0.3 to 0.6, WEWF codes show higher robustness against interference with the gradual increase of PLR. When the PLR is 0.5, the SER of 1.406×10^{-3} for MIS WEWF codes is attainable; however, the SER of EWF codes is only 7.17×10^{-3}. Thus, the WEWF codes can provide better protection for important information in a harsh communication environment.

Decoding Success Rate (DSR). Decoding Success Rate (DSR) is the ratio of the number of successful decoding instances

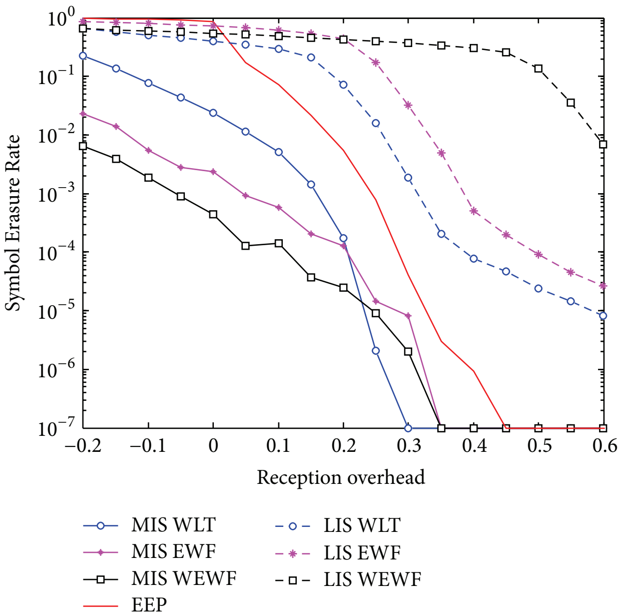

Figure 4: Comparison of SER varied with overhead.

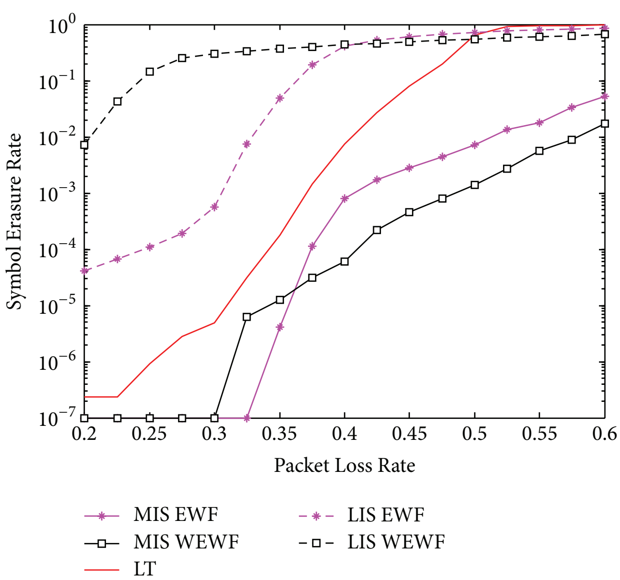

Figure 5: Comparison of SER varied with Packet Loss Rate.

and the total number of simulations. This paper introduces the DSR as the performance metrics to compare the MIS and LIS performance of the three UEP LT codes under the various PLR. In the following simulations, the input symbols length of 1000 and transmission overhead of $E = 2.0$ are employed for fair comparisons.

Figure 6 depicts the DSR of three kinds of UEP LT codes versus PLR. For MIS, their DSRs all approximately approach 1, once the PLR is smaller than 0.4. With the increase of PLR, the DSR of WLT codes declines rapidly. For example, the DSR of 0.038 is attainable at the 0.525 level for PLR; nevertheless, the DSRs of EWF and WEWF codes are just 0.8628 and 0.9076, respectively. Thus, our proposed method is more

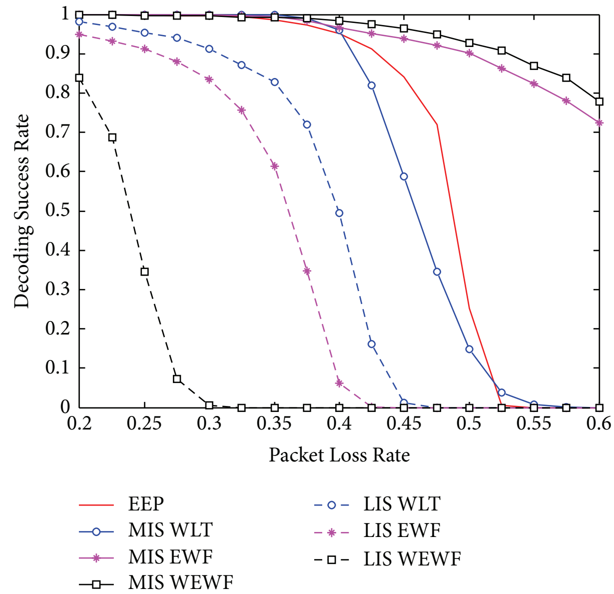

Figure 6: Comparison of DSR varied with Packet Loss Rate.

superior with applications to underwater communication environment.

Based on the above analysis of Figures 4, 5, and 6, a conclusion could be drawn where our method performs better in terms of UEP property than WLT and EWF codes; unfortunately, the improvement of MIS performance is at the expense of the lower prioritized segments. Therefore, the introduction of a feedback scheme to optimize our method is a promising solution for practical applications.

The Overall Redundancy Distribution. Figure 7 shows the overall redundancy distribution of WEWF codes under different feedback schemes. The overall redundancy distribution is a statistical result of the transmission overhead. WEWF codes without feedback need an average overhead of 1.7306 to achieve successful decoding, while, with the intermediate feedback scheme in [9], the required overhead reduces to 1.1199 and the proposed CCFB scheme further put overhead towards 1.0871. The above results confirm that the redundancy in lower prioritized segments can be reduced significantly by the introduction of feedback schemes.

Aiming at further optimizing the transmission strategy using Correlation Chain Feedback, low redundancy data transmission scheme based on DFC is proposed to utilize the aforementioned modified strategies. To demonstrate this feasibility of the proposed scheme for UASNs, a comprehensive performance analysis in terms of the end-to-end delay, network throughput, average transmission redundancy, and the number of retransmissions is performed by the UASN model established on OPNET modeler. The corresponding simulation parameters are provided in Table 1.

End-to-end delay is the data transmission time from the source node to the destination node. Network throughput is used to characterize the channel utilization rate of the transmission scheme. The higher the throughput, the better the

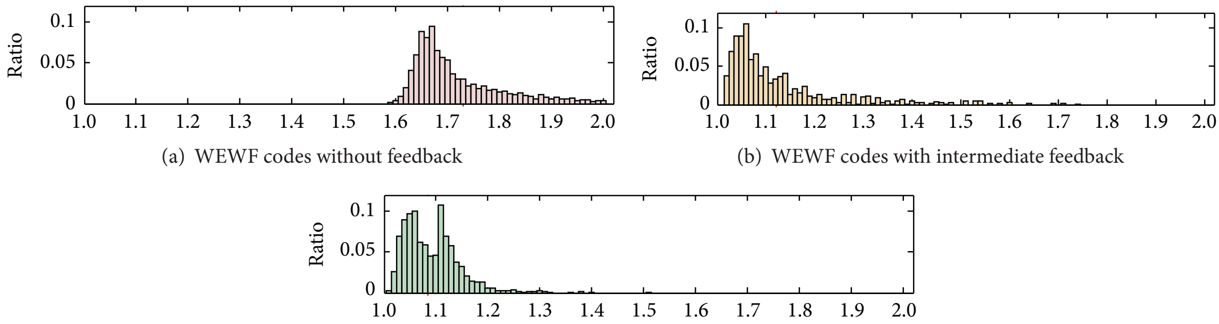

(a) WEWF codes without feedback

(b) WEWF codes with intermediate feedback

(c) WEWF codes with Correlation Chain Feedback

FIGURE 7: Comparison of the overall redundancy varied with feedback schemes.

TABLE 1: Simulation parameter settings.

Parameter name	Symbol	Value
Number of source blocks	K	100
Size of a source block	l	256 (bits)
Transmitting source level	P	166 (dB)
Transmission hop	h	6
Packet sending rate	pk_s	1024 (bps)
Retransmission timeout		
Waiting time	RTO	10
The max transmission range	$l\_\text{range}_{\max}$	3 (km)
Transmission and receipt		
Delay	TR_delay	1 (s)
Band	B	10 (kHz)
The minimum frequency	$f_{\min}$	3 (kHz)
Modulation mode	Modulation Mode	Fsk2

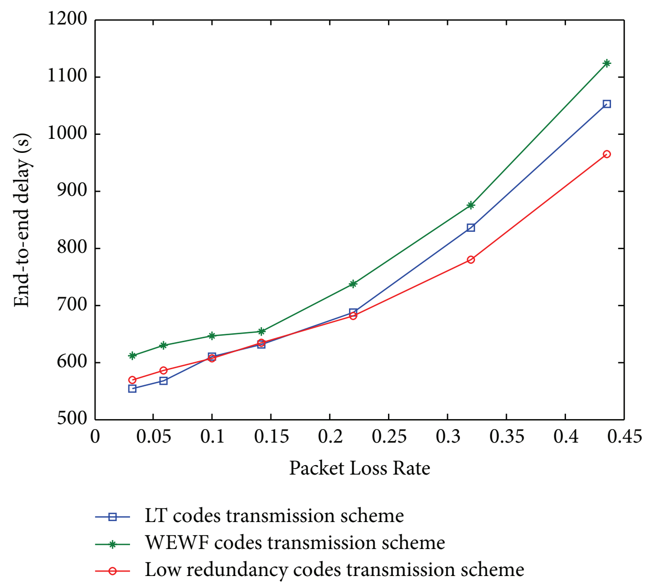

FIGURE 8: End-to-end delay of three kinds of transmission schemes.

utilization rate of the channel. Let pk_delay_i be transmission delay of the ith hop. Then, the network throughput is defined as

$$\text{Throughput} = \frac{K \times l \times h}{\sum_{i=1}^{h} \text{pk\_delay}_i}. \quad (5)$$

Average transmission redundancy and the number of retransmissions are particularly important parameters to characterize the encoding efficiency of the transmission scheme. The lower the efficiency and the number of retransmissions, the higher the transmission efficiency of the corresponding transmission scheme. The definitions of average transmission redundancy and the number of retransmissions are given as follows:

$$\text{Overhead} = \frac{\sum_{i=1}^{h} (\text{pk\_num}_i - K)}{h \times K},$$
$$\text{times} = \frac{\sum_{i=1}^{h} \text{retrans\_}t_i}{h}. \quad (6)$$

End-to-End Delay and Network Throughput. Figure 8 depicts end-to-end delay of all investigated transmission schemes versus PLR. Obviously, with the growth of PLR from 0.32 to 0.44, the end-to-end delay increases by 25.8% for LT codes transmission scheme; it has better channel adaption ability compared with the low redundancy data transmission scheme with the improvement of 23.8% at the same condition. The transmission delay of LT codes and WEWF codes is 836 s and 874.4 s, respectively, for the PLR of 0.32, while that of low redundancy data transmission scheme is 778.9 s which is less than LT codes by 6.8%. The end-to-end delay performance of the three schemes has a perfect agreement with the rule that the low redundancy data transmission scheme is the best, followed by the LT codes and the WEWF codes scheme. The network throughput of the three schemes is also consistent with this rule, shown in Figure 9.

Although the WEWF codes can achieve the UEP property by sacrificing the performance of LIS, we set up the priority of data and did not simulate auxiliary decoding in this chapter; WEWF code will increase decoding delay of LIS when MIS is decoded firstly and it will lead to the increase of the transmission delay of all the system. The introduction of the

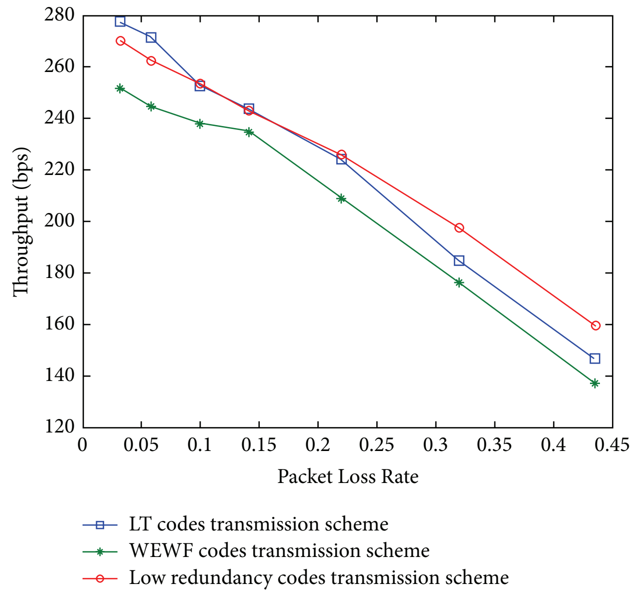

Figure 9: Throughput of three kinds of transmission schemes.

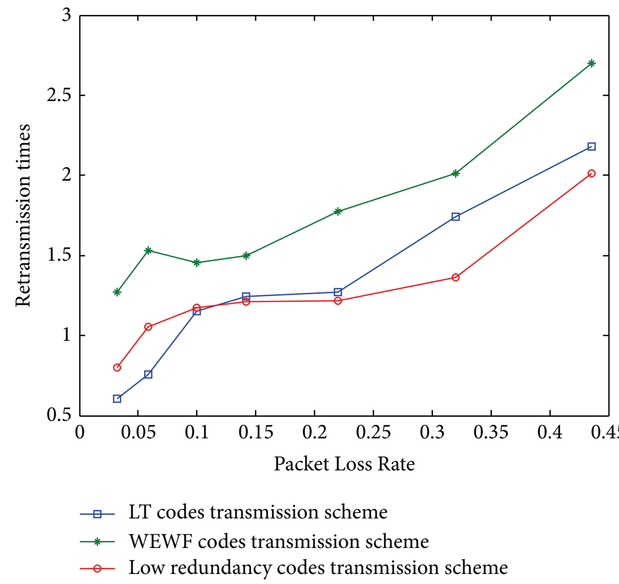

Figure 11: The number of retransmissions under different transmission schemes varied with Packet Loss Rate.

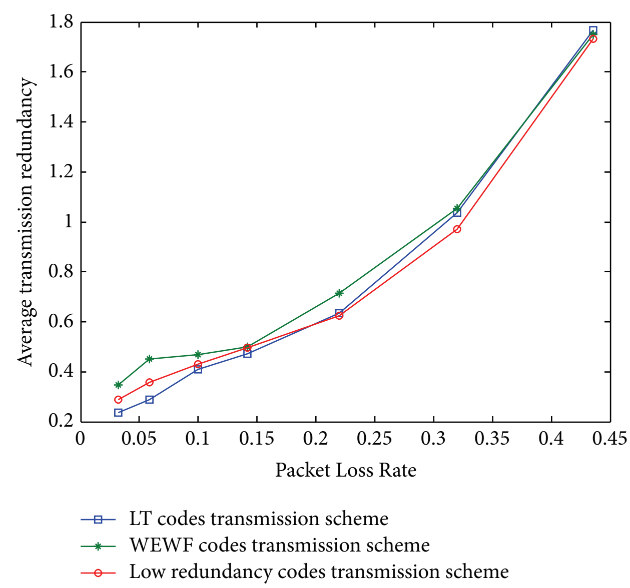

Figure 10: Average transmission redundancy under different transmission schemes varied with Packet Loss Rate.

Correlation Chain Feedback (CCFB) helps the transmitter to precisely adjust the encoding scheme in low redundancy data transmission scheme, which substantially promotes the performance of LIS so that the end-to-end delay and throughput of the whole system are also improved. Therefore, the low redundancy data transmission scheme can achieve lower delay and higher throughput and is more suitable for the harsh communication environment compared with LT codes schemes.

Average Transmission Redundancy and the Number of Retransmissions. Figure 10 shows the average transmission redundancy under various transmission schemes. Due to the significant price in terms of redundancy for the lower prioritized segments, the average transmission redundancy is very high. As is shown in Figure 10, the proposed method improves the overall transmission performance efficiently by introducing the Correlation Chain Feedback (CCFB). As the PLR continues to increase, the average transmission redundancy of the three schemes also goes up. Some small differences between LT codes scheme and lower redundancy data scheme could be observed for the quite low PLR. However, the increased rate of LT codes is particularly more outstanding than the lower redundancy data scheme. As the PLR increases further, the number of lost packets is still going up for such schemes, whereas the lower redundancy data scheme is more effective for performing decoding successfully with fewer packets. These properties make the lower redundancy data scheme helpful in presenting better transmission performance under a terrible communication channel.

Figure 11 depicts the simulation results of the number of retransmissions under diverse transmission schemes. As seen from this figure, the retransmission time is increasing with the growth of PLR for the three considered schemes. The low redundancy data scheme with CCFB can be more targeted to receive information, while improving the successful decoding ratio and reducing the redundancy of the whole system. At the same time, the average retransmission time of low redundancy scheme is also less than those of other schemes because CCFB is more effective than UW-HARQ. For example, the number of retransmissions of low redundancy data scheme is 1.364 which is less than of LT codes scheme by 21.7% for the PLR of 0.32. Moreover, the time of the low redundancy data scheme is also even 7.65% less than of LT codes scheme when the PLR is 0.44 and a harsh communication environment is considered. Thus, encoding efficiency and transmission efficiency of the low redundancy data scheme are both better than of the LT codes scheme, which provides an opportunity for the proposed scheme with applications to complex underwater communication environment.

4. Conclusion

Aiming at the image or video transmission in underwater sensor network, this paper proposes a novel UEP scheme, constructed by the combination of WLT and EWF. The proposed scheme can improve the performance of UEP property effectively, and a feedback scheme called CCFB is also introduced to optimize the performance of the lower prioritized segments. Simulation results demonstrate that the proposed method achieves better performance than the existing schemes.

Competing Interests

The authors declare that there are no competing interests regarding the publication of this manuscript.

Acknowledgments

This paper is funded by the International Exchange Program of Harbin Engineering University for Innovation-Oriented Talents Cultivation. This paper is also supported by the National Natural Science Foundation of China (NSFC), Grant no. 61371099.

References

[1] S. Cai, Z. Gao, D. Yang, and N. Yao, "A network coding based protocol for reliable data transfer in underwater acoustic sensor," *Ad Hoc Networks*, vol. 11, no. 5, pp. 1603–1609, 2013.

[2] D. Zhao, M. Liang, and J. Duan, "Survey of fountain codes in underwater acoustic sensor networks," *Systems Engineering and Electronics*, vol. 36, no. 9, pp. 1838–1843, 2014.

[3] I. F. Akyildiz, D. Pompili, and T. Melodia, "Underwater acoustic sensor networks: research challenges," *Ad Hoc Networks*, vol. 3, no. 3, pp. 257–279, 2005.

[4] M. Luby, "LT codes," in *Proceedings of the 43rd Annual IEEE Symposium on Foundations of Computer Science*, pp. 271–280, November 2002.

[5] A. Shokrollahi, "Raptor codes," *IEEE Transactions on Information Theory*, vol. 52, no. 6, pp. 2551–2567, 2006.

[6] F. C. Zhang, X. Y. Duan, and M. Dong, "Construction of LT codes with unequal erasure protection for rateless data transmission," in *Proceedings of the 10th IEEE and IFIP International Conference on Wireless and Optical Communications Networks (WOCN '13)*, pp. 1–5, Bhopal, India, July 2013.

[7] N. Rahnavard, B. N. Vellambi, and F. Fekri, "Rateless codes with unequal error protection property," *IEEE Transactions on Information Theory*, vol. 53, no. 4, pp. 1521–1532, 2007.

[8] D. Sejdinović, D. Vukobratović, A. Doufexi, V. Šenk, and R. J. Piechocki, "Expanding window fountain codes for unequal error protection," *IEEE Transactions on Communications*, vol. 57, no. 9, pp. 2510–2516, 2009.

[9] S. Ahmad, R. Hamzaoui, and M. M. Al-Akaidi, "Unequal error protection using fountain codes with applications to video communication," *IEEE Transactions on Multimedia*, vol. 13, no. 1, pp. 92–101, 2011.

[10] C. Ni, C. Hou, and W. Xiang, "A novel UEP scheme based upon rateless codes," in *Proceedings of the IEEE Wireless Communications and Networking Conference (WCNC '12)*, pp. 592–596, Shanghai, China, April 2012.

[11] J. H. Sorensen, P. Popovski, and J. Ostergaard, "UEP LT codes with intermediate feedback," *IEEE Communications Letters*, vol. 17, no. 8, pp. 1636–1639, 2013.

[12] J. H. Sorensen, P. Popovski, and J. Ostergaard, "Feedback in LT codes for prioritized and non-prioritized data," in *Proceedings of the IEEE Vehicular Technology Conference (VTC Fall '12)*, vol. 1, pp. 3–6, 2012.

[13] J. H. Sørensen, T. Koike-Akino, and P. Orlik, "Rateless feedback codes," in *Proceedings of the IEEE International Symposium on Information Theory (ISIT '12)*, pp. 1767–1771, July 2012.

[14] L. Zhang, J. Liao, J. Wang, T. Li, and Q. Qi, "Design of improved Luby transform codes with decreasing ripple size and feedback," *IET Communications*, vol. 8, no. 8, pp. 1409–1416, 2014.

[15] T. Ying, L. Xie, and H. Chen, "A novel rateless coding scheme with gradually incremental degree under feedback," in *Proceedings of the IEEE 11th Consumer Communications and Networking Conference (CCNC '14)*, pp. 575–580, Las Vegas, Nev, USA, January 2014.

[16] M. G. Luby, M. Mitzenmacher, and M. A. Shokrollahi, "Analysis of random processes via and-Or tree evaluation," in *Proceedings of the 9th Annual ACM SIAM Symposium on Discrete Algorithms*, pp. 364–373, San Francisco, Calif, USA, 1998.

[17] N. Rahnavard and F. Fekri, "Generalization of rateless codes for unequal error protection and recovery time: asymptotic analysis," in *Proceedings of the IEEE International Symposium on Information Theory (ISIT '06)*, pp. 523–527, IEEE, Seattle, Wash, USA, July 2006.